

elastomer. For CO<sub>2</sub>, predominant sorption was noted with the phenolic spheres. For H<sub>2</sub>O, a major interaction also occurred with the phenolic spheres, and it was much more rapid (< 10 min, compared with 3–4 hr for CO<sub>2</sub>). The silica fibers sorbed water more slowly than did the phenolic spheres, but they sorbed about the same amount of H<sub>2</sub>O.

Component and composite sorption are compared in Table 2. Approximately 85% of the total He sorbed is due to interaction of He with the silica spheres, and the balance, with the phenolic spheres. The saturation pressure obviously must be about the same in the two cases in order to make valid comparisons. The question arises: can the sorption of a given gas by the ablator be treated as a simple sum of the sorption by the components? Interpolation of the results in Fig. 4 gives  $3.10 \times 10^{-6}$  moles of He sorbed per gram of ablator at 200 torr. It is significant that the sum of the component interactions is in excellent agreement with this value as shown in Table 2. Similar agreement with respect to the additivity principle is seen for CO<sub>2</sub>. For H<sub>2</sub>O sorption, however, comparisons of either the extent of component interactions or of the component interactions with the ablator are not possible, since it is experimentally difficult to adjust initial pressures in the technique used such that equivalent saturation pressures are obtained.

The mechanism of He interaction with the silica spheres, and of CO<sub>2</sub> with phenolic spheres, were demonstrated in additional experiments in which crushed silica and phenolic spheres, respectively, were used. Sorption of He on the crushed glass spheres was negligible (Fig. 7). The mechanism of He sorption on the silica spheres then involves simply the diffusion of He through the walls. The diffusion of He through glass is a well-documented phenomenon.<sup>4</sup> The story is different for CO<sub>2</sub> and the crushed and uncrushed phenolic spheres, also shown in Fig. 7. The two curves may approach the same limit at long time, but over 2–3 hr the sorption of CO<sub>2</sub> on crushed phenolic spheres is greater than on the uncrushed phenolic spheres; hence the CO<sub>2</sub> must interact with the bulk phenolic resin represented by the annuli of the hollow spheres. However, diffusion of CO<sub>2</sub> does occur from the interface to the bulk resin and hence the long time necessary to saturate the sample. We have indeed shown<sup>5</sup> that it is possible to obtain the infrared spectrum of the sorbed CO<sub>2</sub> in the phenolic resin. The interaction of CO<sub>2</sub> with the silicone elastomer was not established.

The mechanism of water interaction with the phenolic spheres, silica fibers and silica spheres was not unambiguously established. However, the rapid decrease in water vapor pressure on exposure to the phenolic spheres suggests physisorption of water. The somewhat slower decrease in water vapor pressure on exposure to the silica fibers may be due to physisorption in the small pores of the silica fibers. The different amounts of water sorbed by the ablator at 5- and 30-min intervals are consistent with the time difference observed in the case of the phenolic spheres and the silica fibers.

### References

- <sup>1</sup> Mugler, J. P., Jr. et al., "In Situ Vacuum Testing—A Must for Certain Elastomeric Materials," *Journal of Spacecraft and Rockets*, Vol. 6, No. 2, Feb. 1969, pp. 219–221.
- <sup>2</sup> Brunauer, S., *The Adsorption of Gases and Vapors*, Princeton Univ. Press, Princeton, N.J., 1945, pp. 14–19.
- <sup>3</sup> Orr, C. Jr. and Dallavalle, J. M., *Fine Particle Measurement: Size, Surface and Pore Volume*, Macmillan, New York, 1959, pp. 198–200.
- <sup>4</sup> Dushman, S., *Scientific Foundations of Vacuum Technique*, 2nd ed., Wiley, New York, 1962, p. 676.
- <sup>5</sup> Akers, F. I. and Wightman, J. P., "Absorption of CO<sub>2</sub> by Phenolic Resin," *Journal of Applied Polymer Science*, Vol. 14, No. 1, Jan. 1970, pp. 241–243.

## Scale Modeling Considerations for Thermal Control Coatings

R. K. MACGREGOR  
Renton, Wash.

AND

R. K. THOMPSON\*  
University of Washington, Seattle, Wash.

### Nomenclature

$H, W$  = characteristic dimensions in the  $x$  and  $y$  directions  
 $k$  = thermal conductivity  
 $L$  = model scale ratio; e.g.,  $L = H_m/H_p$   
 $q$  = heat transfer  
 $R$  = thermal resistance  
 $t$  = material thickness ( $z$  direction)  
 $T$  = temperature  
 $x, y, z$  = coordinate directions

### Subscripts

$c, s$  = coating and substrate, respectively  
 $m, p$  = scale model and prototype, respectively

### Introduction

EXTENSIVE studies into the development of scale modeling criteria and the application of scale modeling techniques to spacecraft systems have been presented.<sup>1–4</sup> Recent studies have delved into the limitations inherent in scale modeling due to material and gage availabilities and uncertainties in thermophysical properties.<sup>5,6</sup> These studies have pointed out certain problem areas in the application of scale modeling techniques. One problem, considered herein, relates to the thickness of the thermal control coatings that are used to control radiant heat transfer on the spacecraft. For most solar reflecting coatings, the thickness (typically 10 mils) must be maintained in order to preserve the radiative properties of the surface. In the scale models this preservation of coating thickness significantly affects the heat conduction balance. The temperature errors induced in scale models as a result of preserving the coating thickness and a technique for over-scaling the substrate to offset coating effects, are discussed in this Note.

### Discussion

Consider a thermal control coating of thickness  $t_c$  applied to a substrate panel of dimension  $H \times W \times t_s$ , as measured in the  $x$ ,  $y$ , and  $z$  directions, respectively. The thermal resistance for heat transfer normal to the substrate and coating (in the  $z$  direction) may be expressed as

$$R = (k_{cs}t_s + k_{sc}t_c)/t_{cs}HW \quad (1)$$

Ratioing the thermal resistance for a scale model to that of the prototype configuration results in the equation

$$R_m/R_p = (H_p W_p / H_m W_m) [t_{csp}/t_{csm}] \times [(k_{csm}t_{sm} + k_{scm}t_{cm}) / (k_{csp}t_{sp} + k_{scp}t_{cp})] \quad (2)$$

If the model is constructed with rigid adherence to the three-dimensional scaling criteria as discussed in Refs. 1–5, where  $L = H_m/H_p = W_m/W_p = k_{sm}/k_{sp} = t_{sm}/t_{sp} = k_{cm}/k_{cp} = t_{cm}/t_{cp}$ , then the ratio of thermal resistances reduces to

$$R_m/R_p = 1/L^2 \quad (3)$$

Received March 13, 1970; revision received May 11, 1970. Portions of the work presented here were performed for NASA-Marshall Space Flight Center under Contract NAS8-21422.

\* Coordinator of Special Studies, Office of the Vice-President for Planning and Budgeting.

If, however, the substrate is scaled and the coating conductivity and thickness are preserved, Eq. (2) still reduces to Eq. (3). It is apparent that if all heat conduction occurs in the normal ( $z$ ) direction, no special consideration must be taken when the coating conductivity and thickness are preserved.

The thermal resistance to conduction heat transfer along the surface ( $x$  direction) may be expressed as

$$R = H/W(k_{st_s} + k_{ct_c}) \quad (4)$$

so that

$$R_m/R_p = (H_m W_p / H_p W_m)(k_{sp} t_{sp} + k_{cp} t_{cp}) / (k_{sm} t_{sm} + k_{cm} t_{cm}) \quad (5)$$

If the model is again constructed with a rigid adherence to the three-dimensional scaling criterion, Eq. (5) again reduces to Eq. (3). However, if the substrate is scaled while  $t_c$  and  $k_c$  are preserved, Eq. (5) reduces to

$$R_m/R_p = 1 + (k_{cp} t_{cp} / k_{sp} t_{sp}) / [L^2 + (k_{cp} t_{cp} / k_{sp} t_{sp})] \quad (6)$$

Since  $R_s = H/k_{st_s}W$ , and  $R_c = H/k_{ct_c}W$ , so that

$$R_s/R_c = k_{ct_c}/k_{st_s} \quad (7)$$

Eq. (6) can be expressed as

$$R_m/R_p = (1 + R_{sp}/R_{cp}) / (L^2 + R_{sp}/R_{cp}) \quad (8)$$

The heat conduction ratio is

$$q_m/q_p = R_p \Delta T_m / R_m \Delta T_p \quad (9)$$

but the three-dimensional criterion requires that the energy fluxes be scaled by the square of the scaling ratio. As strict scaling requirements have been compromised, we use this information to calculate the temperature differences which

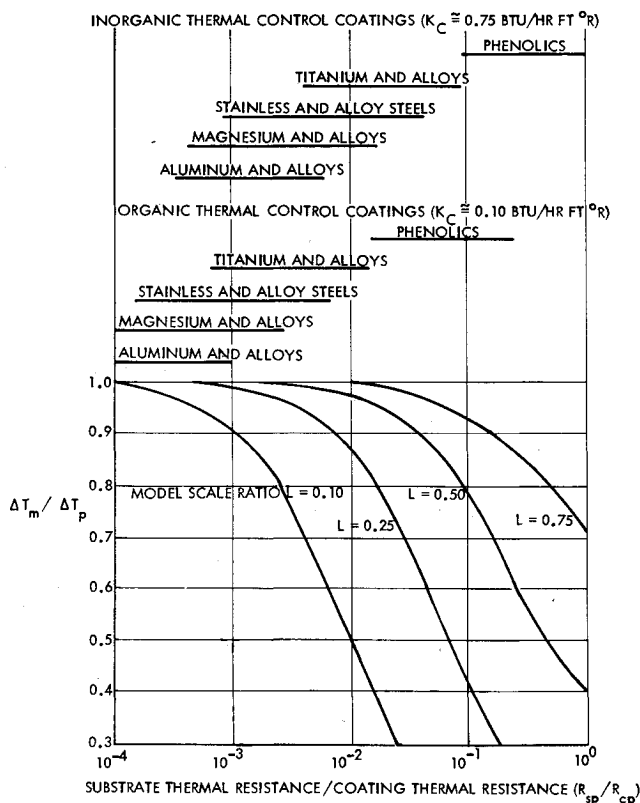


Fig. 1 Temperature errors resulting from failure to scale thermal control coatings, and ranges of thermal resistance ratios for various materials and thermal control coatings.

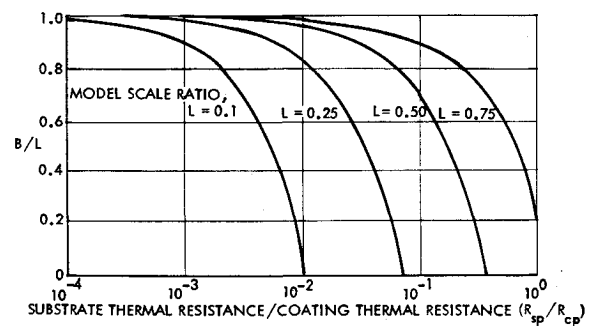


Fig. 2 Substrate requirements to compensate for failure to scale thermal control coatings.

might result. The three-dimensional criterion requires that

$$\Delta T_m / \Delta T_p = L^2 R_m / R_p \quad (10)$$

which reduces, with the substitution of Eq. (8), to

$$\Delta T_m / \Delta T_p = (1 + R_{sp}/R_{cp}) / [1 + (1/L^2)(R_{sp}/R_{cp})] \quad (11)$$

Figure 1 is a plot of Eq. (11) illustrating the temperature differences which occur for several selected scaling ratios. Figure 1 also illustrates the range of the abscissa over which selected combinations of substrate materials and coatings would vary. Coatings which are typical of these two classes are the inorganic Z-93 (developed at Illinois Institute of Technology) and the organic B-1060 (developed at Boeing) thermal control coatings. Both are applied in approximately 10-mil thicknesses (with radiative properties being thickness dependent) and both are white, low  $\alpha_s/\epsilon$  coatings. The nominal thickness of the substrate ( $t_{sp}$ ) utilized for this parameterization is  $\frac{1}{16}$  in. As  $t_{sp}$  or  $k_{sp}$  increases, the effect of failure to scale the coating becomes less important.

As most spacecraft would be fabricated from a variety of metallic materials, it is evident that models in the range of  $\frac{1}{4}$  to  $\frac{1}{10}$  of full size might incur considerable errors. One solution would be to overscale the substrate, when building a scale model, to compensate for the increased conduction in the coating. If the model is constructed with  $H_m/H_p = W_m/W_p = k_{sm}/k_{sp} = L$ , but  $t_{sm}/t_{sp} = B$ , and  $k_{cm}/k_{cp} = t_{cm}/t_{cp} = 1$ , then Eq. (2) reduces to

$$R_m/R_p = (k_{sp} t_{sp} + k_{cp} t_{cp}) / (B L k_{sp} t_{sp} + k_{cp} t_{cp}) \quad (12)$$

However, if the temperatures and heat transferred both through the coating and substrate are preserved, then Eq. (3) must apply. Therefore, setting the right side of Eq. (11) equal to  $1/L^2$ , using Eq. (7), and rearranging, we obtain

$$B/L = 1 + (R_{sp}/R_{cp})[1 - (1/L^2)] \quad (13)$$

Figure 2 illustrates this relationship for the same range of variables as shown in Fig. 1. Here, however, a definite limitation is imposed on this method of overscaling due to the fact that eventually the coating itself conducts more energy than is permissible for the scaled coating-substrate system. At this point, compensating by this technique would have completely eliminated the substrate material. Thus only the most highly conducting substrates would allow accurate modeling below scale ratios of  $\frac{1}{10}$ .

### Summary

If energy transport normal to surfaces is dominant (energy transport along surfaces negligible), no special consideration must be given to scaling thermal control coatings for steady state response. If energy transport along the surface is not negligible, failure to scale the coating will result in temperature errors as predicted by Eq. (11); the substrate may be overscaled, to compensate for failure to scale the coating, in accordance with Eq. (13).

## References

- <sup>1</sup> Katzoff, S., "Similitude in Thermal Models of Spacecraft," TN D-1631, April 1963, NASA.
- <sup>2</sup> Vickers, J. M. F., "A Study of Thermal Scale Modeling Techniques," TM-33-153, Sept. 1963, Jet Propulsion Lab., Pasadena, Calif.
- <sup>3</sup> Chao, B. T. and Wedekind, G. L., "Similarity Criteria for Thermal Modeling of Spacecraft," *Journal of Spacecraft and Rockets*, Vol. 2, No. 2, Feb. 1965, pp. 146-152.
- <sup>4</sup> Jones, B. P., "Theory of Thermal Similitude with Applications to Spacecraft—A Survey," *Astronautics Acta*, Vol. 12, No. 4, March, 1966, pp. 258-271.
- <sup>5</sup> MacGregor, R. K., "Limitations in Thermal Similitude," D2-121352-1, Final Report on Contract NAS8-21422, Dec. 1969, The Boeing Co., Seattle, Wash.
- <sup>6</sup> Rolling, R. E., "Limitations in Thermal Modeling," LMSC 61-78-69-41, Dec. 1969, Lockheed Missile & Space Co., Sunnyvale, Calif.

## Solar Heating of a Rotating Cylinder with a Conduction Discontinuity

ROBERT J. EBY\* AND ROBERT D. KARAM†  
*Fairchild Hiller Corporation,  
 Space and Electronics Systems Division,  
 Germantown, Md.*

## Nomenclature

$A, B, C$	= dimensionless parameters
$c$	= specific heat
$F, f$	= solar input functions
$G_1, G_2, G_3$	= transform functions defined by Eqs. (13, 14, and 20)
$G(\theta_s)$	= function defined by Eq. (24)
$k$	= thermal conductivity
$r$	= radius
$S$	= solar flux
$t$	= thickness
$T$	= absolute temperature
$\alpha$	= solar absorptance
$\epsilon$	= emittance
$\eta$	= temperature fluctuation function
$\theta$	= angular position on circumference
$\rho$	= density
$\sigma$	= Stefan-Boltzmann constant
$\tau$	= dimensionless temperature defined by Eq. (4)
$\psi$	= rotational position
$\omega$	= angular speed

## Subscripts

$m$	= mean
$n$	= 1, 2, ...
$s$	= position of solar vector

## Introduction

THE temperature distribution in rotating space vehicles in a solar environment is a subject of considerable engineering importance, and much attention has been given to the corresponding mathematical problems. Previous work on these problems<sup>1,2</sup> has been largely limited to systems in which conduction heat transfer is continuous throughout the solid portion of the body. During a uniform quasi-steady-state rotation of a sphere or a cylinder, the explicit dependence on time may be eliminated by relating time to spatial coordinates.<sup>3</sup> The mathematical model is then generated based on an established, nonchanging temperature profile as observed from a fixed frame of reference.

Received May 15, 1970.

\* Manager, Thermal Control.

† Principal Engineer, Thermal Control.

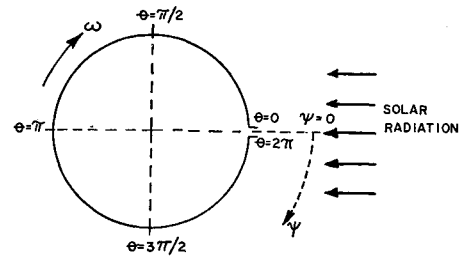


Fig. 1 Coordinate system.

This procedure cannot in general be implemented when the system involves a discontinuity in heat conduction; the temperature distribution will contain the explicit dependence on time as well as the spatial coordinates. In this Note, a thin cylindrical shell with a line conduction discontinuity is considered. The cylinder is rotating at a constant angular speed about the geometric axis which is normal to solar radiation. The temperature distribution is obtained as a function of time and dimensionless groups which include the thermal and geometric parameters. Comparison is made with a similar system which does not include the effects of discontinuous conduction. One direct application to this solution is in the evaluation of thermal bending of tubular extendible elements on spinning spacecrafts. Current designs of these elements incorporate seams of interlocking tabs along which conduction heat transfer is negligible.

## Analysis

Consider an infinitely long thin cylindrical shell of open cross-section rotating uniformly in a solar radiation field as shown in Fig. 1. If it is assumed that 1) the open gap is small and its position with respect to the solar vector does not vary along the length, 2) internal radiation and heat interchange across the gap are negligible, 3) the thermophysical properties are independent of temperature and geometry, and 4) thermal distortions are small, the differential equation which relates heat conduction to the energy received, re-radiated and stored may be written

$$\frac{\partial^2 T}{\partial \theta^2} + \frac{\alpha S r^2}{k t} f(\theta, \psi) - \frac{\epsilon r^2}{k t} \sigma T^4 = \frac{r^2 \rho c \omega}{k} \frac{\partial T}{\partial \psi} \quad (1)$$

with the boundary conditions (assumption 2)

$$\partial T / \partial \theta|_{\theta=0} = 0 \text{ and } \partial T / \partial \theta|_{\theta=2\pi} = 0 \quad (2)$$

Since only quasi-steady-state conditions are considered, the initial temperature may be taken as zero.

The input function  $f(\theta, \psi)$ , which characterizes the rotation of each point  $\theta$  on the periphery with respect to solar radiation, is a rectified cosine wave which is displaced along the time axis by the magnitude of the angle, with  $\theta = 0$  and  $\theta = 2\pi$  defining the edges of the gap. If a delayed function of the form

$$F(\psi - \theta) U(\psi - \theta)$$

where  $F(\psi) = f(0, \psi)$  and  $U(\psi - \theta)$  is 1.0 for  $\psi \geq \theta$  and 0 for  $\psi < \theta$ , is inserted into Eq. (1), then the required quasi-steady state temperature is obtained.

Equation (1) is linearized by introducing the following definitions<sup>1</sup>:

$$T = T_m(1 + \eta) \quad |\eta| \ll 1.0 \quad (3)$$

$$\tau = \eta + \frac{1}{4} \quad (4)$$

where  $\eta$  and  $\tau$  are dimensionless parameters and  $T_m$  is a mean temperature which may be defined by

$$\epsilon \sigma T_m^4 = \frac{1}{2\pi} \int_0^{2\pi} \alpha S f(\theta, \psi_0) d\theta$$